

**Report Title:** Bi-Layer p-n Junction Interconnections for Coal Based Solid Oxide Fuel Cells

**Type of Report:** Final Technical report

**Reporting Period Start Date:** 7/10/03

**Reporting Period End Date:** 10/31/04

**Principal Author:** Srikanth Gopalan

**Dated:** January 29, 2005

**DOE Award Number:** DE-FG26-03NT41800

**Department of Manufacturing Engineering  
15 St. Mary's Street  
Boston University, MA 02446**

Disclaimer: "This report was prepared as an account of work sponsored by an agency of the United States Government. Neither the United States Government nor any agency thereof, nor any of their employees, makes any warranty, express or implied, or assumes any legal liability or responsibility for the accuracy, completeness, or usefulness of any information, apparatus, product, or process disclosed, or represents that its use would not infringe privately owned rights. References herein to any specific commercial product, process, or service by trade name, trademark, manufacturer, or otherwise does not necessarily constitute or imply its endorsement, recommendation, or favoring by the United States Government or any agency thereof. The views and opinions of authors expressed herein do not necessarily state or reflect those of the United States Government or any agency thereof."

## **TABLE OF CONTENTS**

ABSTRACT	3
BI-LAYER INTERCONNECTION	4
THEORETICAL ANALYSIS	5
EXPERIMENTAL WORK TO DATE AND - FUTURE WORK	10
CONCLUSIONS	11
REFERENCES	11
FIG. 1: BI-LAYER INTERCONNECT ELEMENT	14
FIG. 2: SPECIES TRANSPORT DIRECTION IN BI-LAYER INTERCONNECTION	15
FIG. 3: VARIATION OF LOG(pO <sub>2</sub> ) VERSUS THICKNESS OF LSM LAYER WITH THE CHANGE OF THE THICKNESS OF AST LAYER	16
FIG. 4: VARIATION OF LOG(pO <sub>2</sub> ) VERSUS THICKNESS OF BI-LAYER LSM-AST INTERCONNECTION	17
FIG.5: VARIATION OF LOG(pO <sub>2</sub> ) VERSUS THICKNESS OF BI-LAYER LSM-AST INTERCONNECTION	18
FIG. 6: EXPERIMENTAL TEST SETUP OF THE BI-LAYER STRUCTURE	19
FIG. 7: CONDUCTIVITY OF BI-LAYER IC AS A FUNCTION OF TEMPERATURE IN AIR AND FORMING GAS	20
FIG.8: SEM CROSS-SECTION OF THE BI-LAYER IC	21

## **ABSTRACT**

In this report, a new approach for lower operating temperature solid oxide fuel cells (SOFCs) interconnections (IC) consisting of a bi-layer structure is proposed and analyzed. The bi-layer structure consists of a p-type layer exposed to cathodic gas (air/oxygen) and an n-type layer exposed to anodic gas (fuel). It is theoretically shown that the interfacial oxygen partial pressure which is an important design variable, is dependent primarily on the oxygen partial pressure gradient across the IC, the low level oxygen conductivities of the two layers and is largely independent of their electronic conductivities and the total current density through the IC material. Experimental difficulties in fabricating bi-layer structures are presently being addressed.

## **1. INTRODUCTION**

Current research on solid oxide fuel cells (SOFCs) is focused on reducing the operating temperature from a nominal temperature of 1000°C to 600-800°C. Reducing the operating temperature allows the use of low-cost stack and manifolding materials, shorter heat up time, and enabling use in small scale residential and transportation applications [1-3]. However, reducing the operating temperature also has the unintended negative consequences of higher electrode polarization, and higher area specific electrolyte and interconnection resistances [4, 5]. In particular doped-LaCrO<sub>3</sub> a high temperature p-type semiconductor which is used as the interconnection material in state-of-the-art high temperature SOFCs is a very poor choice for an interconnection material in the 600-800°C

temperature regime for two different reasons [6-8]. First, the conduction mechanism in doped-LaCrO<sub>3</sub> is small polaron hopping which is a thermally activated process. Thus the p-type conductivity of this material decreases exponentially with decreasing temperature. Secondly, the interconnection material like the solid electrolyte in the SOFC, is exposed to highly oxidizing conditions on the cathodic side ( $p_{O_2} = 0.21$  atm) and highly reducing conditions on the anode side of the where a highly reducing atmosphere ( $10^{-18}$  to  $10^{-21}$  atm) exists. Thus a gradient in the electronic conductivity exists across the interconnect with a high conductivity on the cathode and side and poor conductivity on the anode side leading to an overall low average electronic conductivity across the interconnect. Bilayered electrolyte has been considered for use in SOFC or membranes with the objectives of blocking electronic current, improve open-circuit voltage and increasing interfacial oxygen partial pressure to enhance chemical stability of materials under reducing environment [9-19]. In this paper, we propose and analyze a novel concept for an improved SOFC interconnection structure with a high average conductivity across the entire thickness.

## **2. BI-LAYER INTERCONNECTION**

The new interconnection concept we propose is shown schematically in Fig. 1. The concept we propose consists of a bi-layer structure with one p-type layer and one n-type layer adjacent to each other. In an actual device, the p-type layer of the bi-layer interconnection will be exposed to an oxidizing environment

and the n-type layer exposed to reducing conditions. During operation of the cell, the layer exposed to the cathodic side will develop p-type conductivity and the layer exposed to the anodic side will develop n-type conductivity. If designed correctly, such a structure has the potential to serve as an excellent SOFC interconnection, maintaining a high electronic conductivity across its thickness. In what follows we analyze species transport across the proposed bi-layer interconnection and derive equations that provide design criteria for such a structure.

### 3. THEORETICAL ANALYSIS

Fig. 2 shows a schematic of the bi-layer interconnection and associated transport directions of oxygen ions  $O^{2-}$ , holes  $h^+$  and electrons  $e^-$ . The generalized current density of species 'k' is given by [20],

$$J_k = -\frac{\sigma_k}{z_k e} \nabla \eta_k \quad (1)$$

Applying equation (1) to transport of  $O^{2-}$ ,  $h^+$ , and  $e^-$ , the species current densities can be written as,

$$J_i = \frac{\sigma_i}{2e} \nabla \eta_i \quad (2a)$$

$$J_p = -\frac{\sigma_p}{e} \nabla \eta_p \quad (2b)$$

$$J_n = \frac{\sigma_n}{e} \nabla \eta_n \quad (2c)$$

The sum of the species current densities can then be equated to the total current density through the bi-layer interconnection under SOFC operating conditions, i.e.

$$J = J_i + J_p + J_n \quad (3)$$

The next step in the analysis is the assumption that local thermodynamic equilibrium prevails between neutral oxygen gas, oxygen ions and electrons/holes, i.e. the following reactions are in thermodynamic equilibrium everywhere across the interconnection structure.



Assumption of thermodynamic equilibrium of the above reactions gives,

$$\frac{1}{2} \nabla \mu_{O_2} + 2 \nabla \eta_n = \nabla \eta_i \quad (4)$$

$$\frac{1}{2} \nabla \mu_{O_2} = \nabla \eta_i + 2 \nabla \eta_p \quad (5)$$

$$\nabla \eta_n + \nabla \eta_p = 0 \quad (6)$$

Substituting equations (2), (4), (5) and (6) in (3) it can be shown that,

$$J_{el} = J_n + J_p = \frac{\sigma_n + \sigma_p}{\sigma_i + \sigma_n + \sigma_p} J - \frac{1}{2e} \frac{\sigma_i (\sigma_n + \sigma_p)}{\sigma_i + \sigma_n + \sigma_p} \nabla \mu_{O_2} \quad (7a)$$

$$J_i = \frac{1}{2e} \frac{\sigma_i (\sigma_n + \sigma_p)}{\sigma_i + \sigma_n + \sigma_p} \nabla \mu_{O_2} + \left( \frac{\sigma_i}{\sigma_i + \sigma_n + \sigma_p} \right) J \quad (7b)$$

Each of the above equations (7a) which represents the total electronic current density (electron and hole current density) and (7b) which represents the total ionic current density has two terms. One associated with  $J$  the total external current density and the other  $\nabla \mu_{O_2}$  the gradient in the neutral oxygen chemical potential gradient. The transport coefficient multiplying  $\nabla \mu_{O_2}$ , namely  $\frac{\sigma_i (\sigma_n + \sigma_p)}{\sigma_i + \sigma_n + \sigma_p}$  is easily recognized as the ambipolar conductivity of the individual layers. In general the conductivities  $\sigma_i$ ,  $\sigma_n$  and  $\sigma_p$  will be functions of temperature and composition. Since the composition is both a function of the local electrostatic potential and the oxygen partial pressure, the conductivities are expected to vary as a function of position. In what follows we make relevant

simplifying assumptions to derive analytical expressions that can guide design of the bi-layer interconnection.

Firstly, we assume that the ionic conductivity in the two layers is invariant with  $pO_2$ . Secondly, we assume that the ionic conductivity is much smaller in magnitude than the sum of the electron and hole conductivities, i.e.  $\sigma_i \ll (\sigma_n + \sigma_p)$ . The first assumption is true of most p-type and n-type oxide electronic conductors. In these materials the oxygen ionic conductivity is determined extrinsically, i.e. it is a stronger function of the aliovalent dopant level rather than  $pO_2$ . The second assumption is a necessary condition to be satisfied of any candidate interconnection material. With the second of these assumptions, equations (7) can be simplified to,

$$J_{el} = J - \frac{1}{2e} \sigma_i \nabla \mu_{O_2} \quad (8a)$$

$$J_i = \frac{1}{2e} \sigma_i \nabla \mu_{O_2} \quad (8b)$$

These assumptions imply that at steady state, the current passing through the bi-layer interconnection is substantially electronic in nature. Further the rather small oxygen ionic current through the bi-layer given by equation (8b) does not depend on the total current through the interconnection but only on the cathodic and anodic side  $pO_2$ 's. Assuming that the chemical and electrostatic potential gradients are one-dimensional and integrating equation (8b) over both layers it can be shown that,

$$J_{i1} = \frac{k_B T \sigma_{i1}}{2e \delta_1} \ln \left[ \frac{pO_2(c)}{pO_2(i)} \right] \quad (9a)$$

$$J_{i2} = \frac{k_B T \sigma_{i2}}{2e \delta_2} \ln \left[ \frac{pO_2(i)}{pO_2(a)} \right] \quad (9b)$$

The interfacial oxygen partial pressure  $pO_2(i)$  which is an important design parameter as will be seen shortly can be derived by equating the ionic current densities through the two layers at steady state, i.e.  $J_{i1} = J_{i2}$ , i.e.

$$pO_2(i) = \left[ \{pO_2(c)\}^{\frac{\sigma_{i1}}{\delta_1}} \{pO_2(a)\}^{\frac{\sigma_{i2}}{\delta_2}} \right]^{\frac{1}{\frac{\sigma_{i1}}{\delta_1} + \frac{\sigma_{i2}}{\delta_2}}} \quad (10)$$

Equation (10) gives the interfacial oxygen partial pressure as a function of the oxygen partial pressure on the cathodic and anodic sides, the oxygen ionic conductivities in the two regions and the thickness of the two layers.

Considering the match of thermal expansion coefficient (TEC) and high electrical conductivity,  $La_{1-x}Sr_xMnO_{3-\delta}$  (LSM) is selected as p-type layer, n-type layer is A site donor doped  $SrTiO_3$  (AST) [21,22]. As literature suggests:  $\sigma_{i,LSM}=10^{-7}$  S/cm,  $\sigma_{i,AST}=10^{-5}$  S/cm at 900°C [23-25], assuming  $pO_2(c)=0.21$ atm,  $pO_2(a)=10^{-18}$ atm, substitute these data into equation (10) to calculate the interfacial oxygen partial pressure as a function of the thickness of the two layers, which was displayed in Fig.3. Fig. 4 shows the variation of  $\log(pO_2)$  versus

thickness of bi-layer LSM-AST interconnection at 900°C,  $pO_2(c)=0.21\text{atm}$ ,  $pO_2(a)=10^{-18}\text{atm}$ . The interconnection design criterion is  $pO_2(i) > pO_2^*$ , where  $pO_2^*$  is the decomposition  $pO_2$  for the p-type materials. Fig. 5 shows that for a given pair of p-type (LSM) and n-type (AST) materials, by carefully choosing the thickness of the two layers, one can in principle ensure that the interfacial oxygen partial pressure remains higher than the decomposition partial pressure for the p-type layer.

#### 4. Experimental work to date and future work

$\text{La}_{1-x}\text{Sr}_x\text{MnO}_{3-\delta}$  (LSM) specimens with 15mol%  $\text{Sr}_2\text{O}_3$  and  $\text{Y}_{1-x}\text{Sr}_x\text{Ti}_{1-y}\text{Al}_y\text{O}_3$  (AST) specimens with 8mol%  $\text{Y}_2\text{O}_3$  and 5mol%  $\text{Al}_2\text{O}_3$  were used in the present work. Powder used to produce the specimens was prepared by conventional solid-state reaction from the oxides. The powder was ball milled after the calcination, and was pressed into pellets. The LSM specimens were sintered in air at 1400 °C for 5hours, while the AST specimens were sintered in forming gas (5% Hydrogen gas and 95% Argon gas) at 1450 °C for 10 hours. The specimens were polished to 1 $\mu\text{m}$  using SiC polishing paper and  $\text{Al}_2\text{O}_3$  polishing suspension. Diffusion bonding of sintered compacts of LSM and AST was carried out at 1400 °C for 5 hours in air.

The bi-layer samples were tested in dual atmosphere (one side is air and the other side is forming gas bubbling through water at room temperature). The bi-layer test setup is shown in Fig.6. Fig.7 shows the conductivity of the bi-layer IC as a function of temperature in air and forming gas. Fig. 8 shows the cross

section SEM of the bi-layer IC. The contact between LSM/AST bi-layers formed by this technique is not continuous, thus measured conductivity values are not representative potential conductivity of bi-layer structures. In phase-II deposition of p-type LSM films on AST substrates will be achieved through PLD and the conductivity measurements will be repeated.

## 5. Conclusions

The requirements for the bi-layer IC is high conductivity and excellent stability in a high oxygen partial pressure gradient. Analysis of bi-layer interconnection structure shows that when  $\sigma_i \ll (\sigma_n + \sigma_p)$ , interfacial  $pO_2$  is independent of  $\sigma_n$  and  $\sigma_p$ . Region with higher  $\sigma_i$  will have a shallower  $pO_2$  distribution. By carefully choosing the thicknesses of the two layers, one can in principle ensure that the interfacial oxygen partial pressure remains higher than the decomposition partial pressure for the p-type layer. More detailed measurements of  $\sigma_i$  as a function of  $pO_2$  required for robust design of bi-layer interconnections. Experimental difficulties in fabricating bi-layer structures are presently being addressed.

## 6. Publications

“Bi-layer structures as solid oxide fuel cell interconnections”, W.Huang and S.Gopalan (Solid State Ionic; accepted for publication)

## References

- [1] S. Souza, S. J. Visco and L. C. D. Jonghe, *Solid State Ionics* 98 (1997) 57.
- [2] C. Xia and M. Liu, *Adv. Mater.* 14 (2002) 521.
- [3] H. Tu and U. Stimming, *J. Power Sour.* 127 (2004) 284.
- [4] M.T. Colomer, B. C. H. Steele and J. A. Kilner, *Solid State Ionics* 147 (2002) 41.
- [5] J. Kim, A. V. Virkar, K. Fung, K. Mehta and S. C. Singhal, *J. Electrochem. Soc.* 146 (1) (1999) 69.
- [6] K. Deshpande, *J. Am. Ceram. Soc.* 86(7) (2003) 1149.
- [7] F. Boroomand, E. Wessel, H. Bausinger, and K. Hilpert, *Solid State Ionics* 129 (2000) 251.
- [8] I. Yasuda and M. Hishinuma, *J. Electrochem. Soc.* 143 (5) (1996) 1583
- [9] H. Yahiro, Y. Baba, K. Eguchi, and H. Arai, *J. Electrochem. Soc.* 135 (1988) 2077.
- [10] A. V. Virkar, *J. Electrochem. Soc.* 138 (1991) 1481
- [11] F. M. B. Marques and L. M. Navarro, *Solid State Ionics* 90 (1996) 183.
- [12] F. M. B. Marques and L. M. Navarro, *Solid State Ionics* 100 (1997) 29.
- [13] T. Tsai, L. Perry and Barnett, *J. Electrochem. Soc.* 144 (5) (1997) 35.
- [14] P. Soral, U. Pal and W. L. Worrell, *J. Electrochem. Soc.* 145 (1) (1998) 99.
- [15] Y. Mishima, H. Mitsuyasu, M. Ohtaki and K. Eguchi, *J. Electrochem. Soc.* 145 (3) (1998) 1004.
- [16] S. H. Chan, X. J. Chen and K. A. Khor, *Solid State Ionics* 158 (2003) 29.

- [17] E. D. Wachsman, P. Jayaweera, N. Jiang, D. M. Lowe and B. G. Pound J. Electrochem. Soc. 144 (1997) 233
- [18] E. D. Wachsman, Solid State Ionics 152-153 (2002) 657.
- [19] E. D. Wachsman and T. L. Clites, J. Electrochem. Soc. 149 (3) (2002) A242.
- [20] L. Heyne in *Solid Electrolytes, Topics in Applied Physics*, S. Geller, Editor, p. 169, Springer, Berlin (1977)
- [21] A. Hammouche, E. Siebert and A. Hammou, Mat. Res. Bull. 24 (1989) 367.
- [22] S. Hui and A. Petric, J. Eur. Ceram. Soc. 22 (2002) 1673.
- [23] I. Yasuda, K. Ogasawara, M. Hishinuma, T. Kawada and M. Dokiya, Solid State Ionics 86-88 (1996) 1197.
- [24] S. Hui and A. Petric, Mat. Res. Bull. 37 (2002) 1215.
- [25] T. Kawada, T. Watanabe, A. Kaimai, K. Kawamura, Y. Nigara and J. Mizusaki, Solid State Ionics 108 (1998) 391.

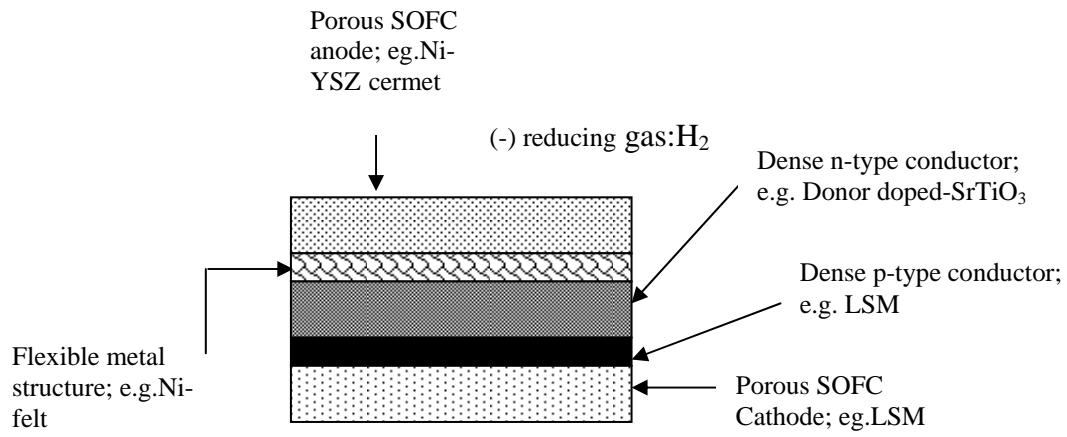


**Figure 1. Bi-layer interconnection element**

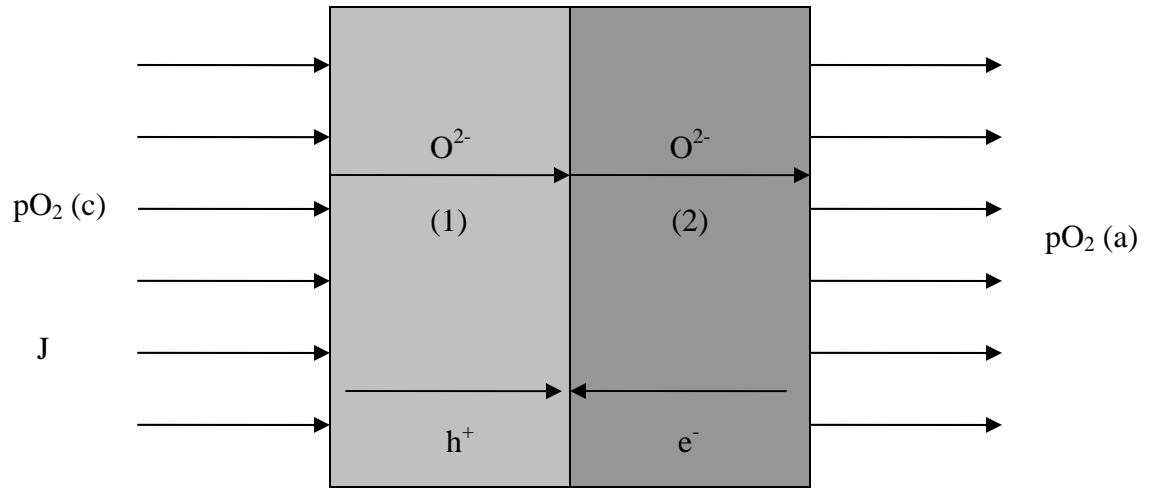
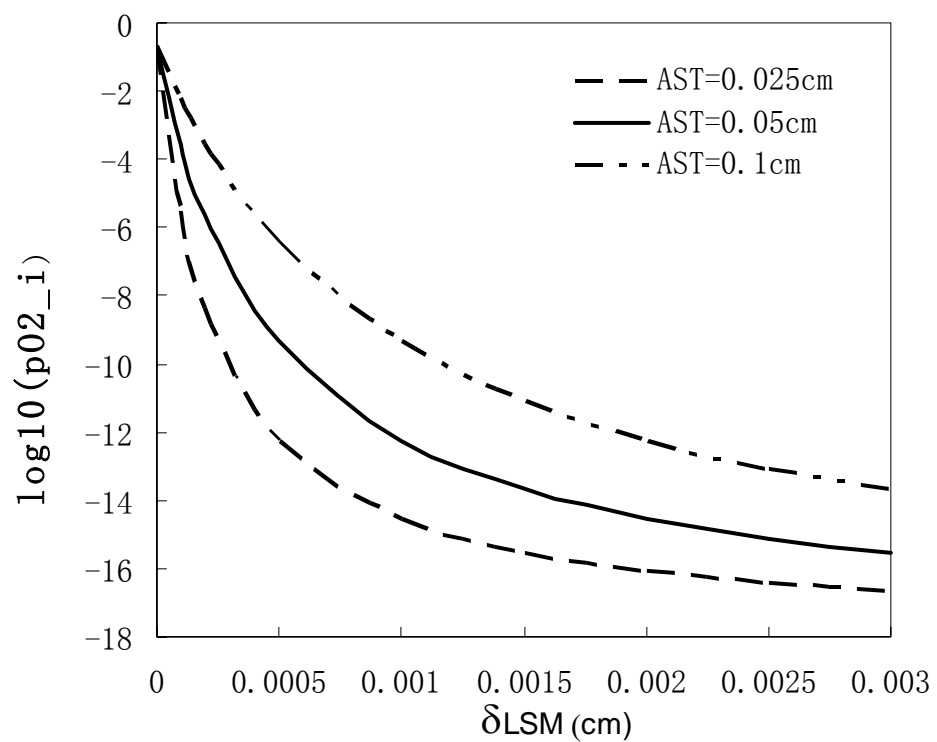
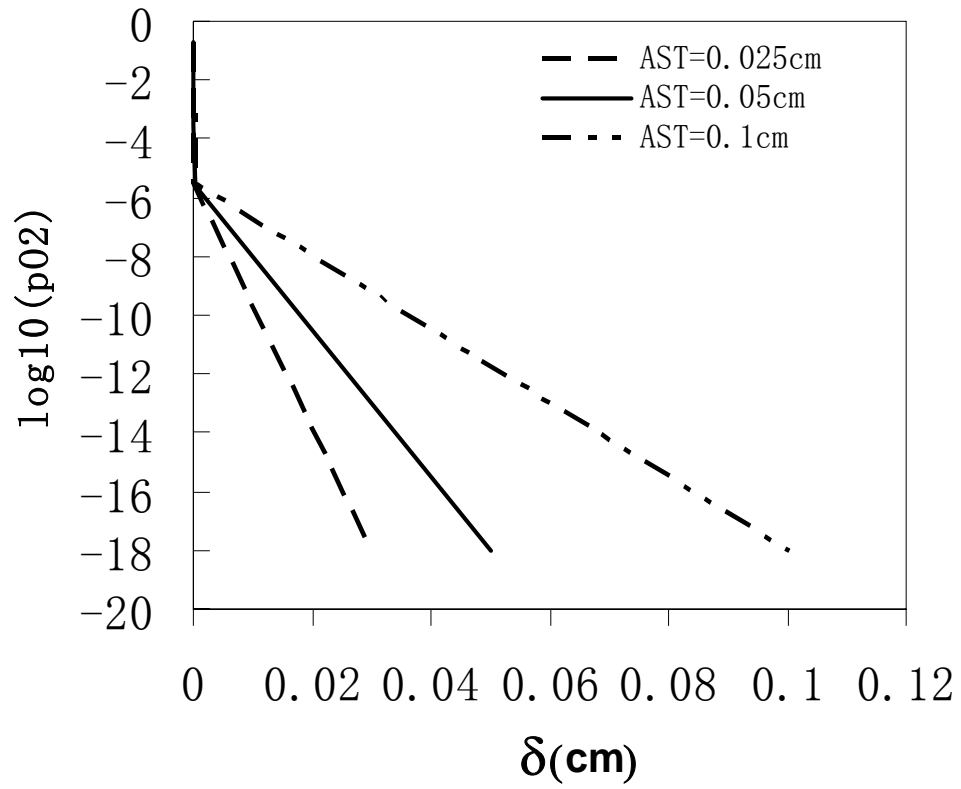


Figure 2. Species transport direction in bi-layer interconnection



**Figure 3. Variation of  $\log(pO_2)$  versus thickness of LSM layer with the change of the thickness of AST layer**



**Figure 4. Variation of  $\log(pO_2)$  versus thickness of bi-layer LSM-AST interconnection**

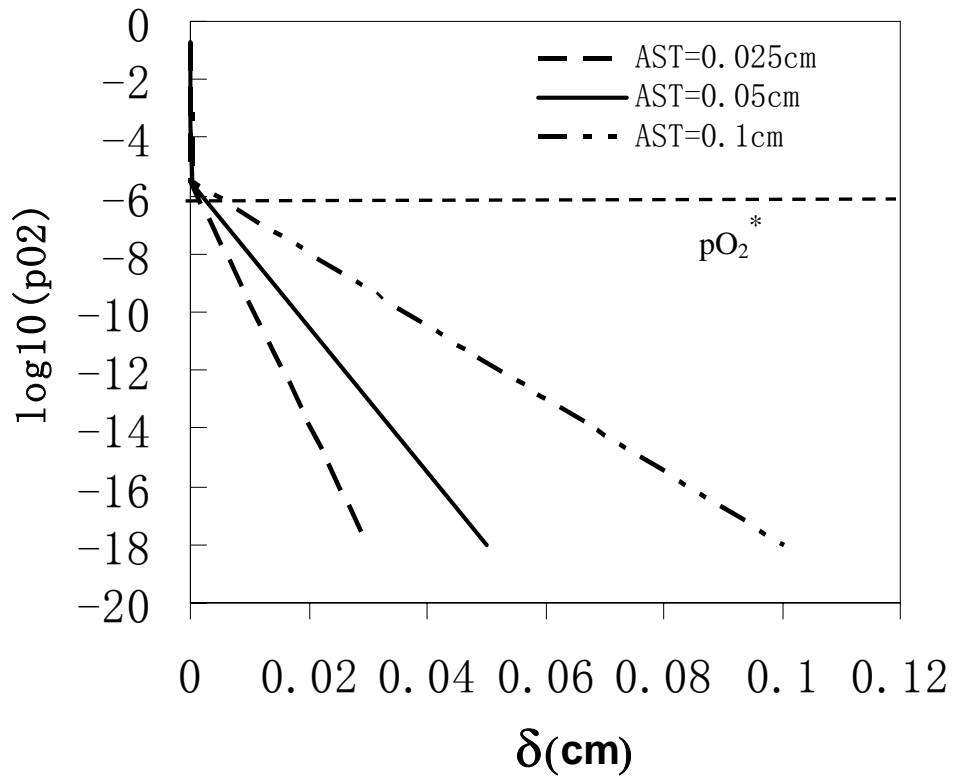


**Figure 5. Variation of  $\log(pO_2)$  versus thickness of bi-layer LSM-AST interconnection**

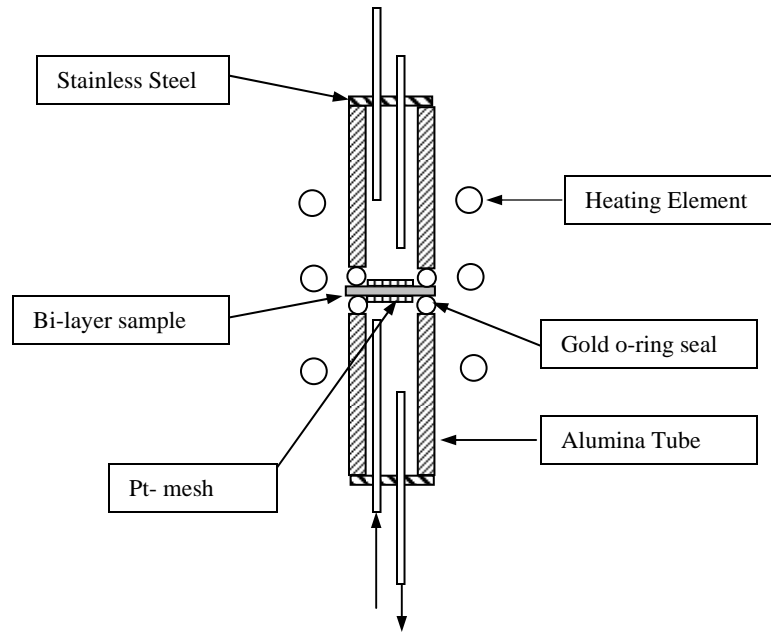


**Figure 6 Experimental test setup of the bi-layer structure**

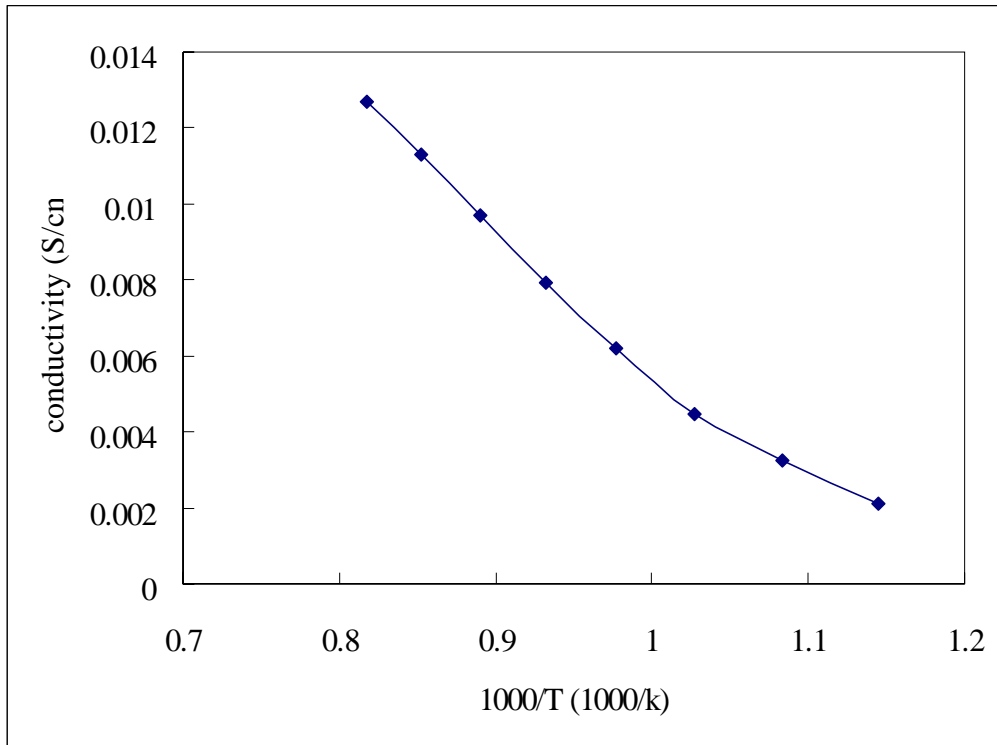


Figure 7 Conductivity of bi-layer IC as a function of temperature in air and forming gas

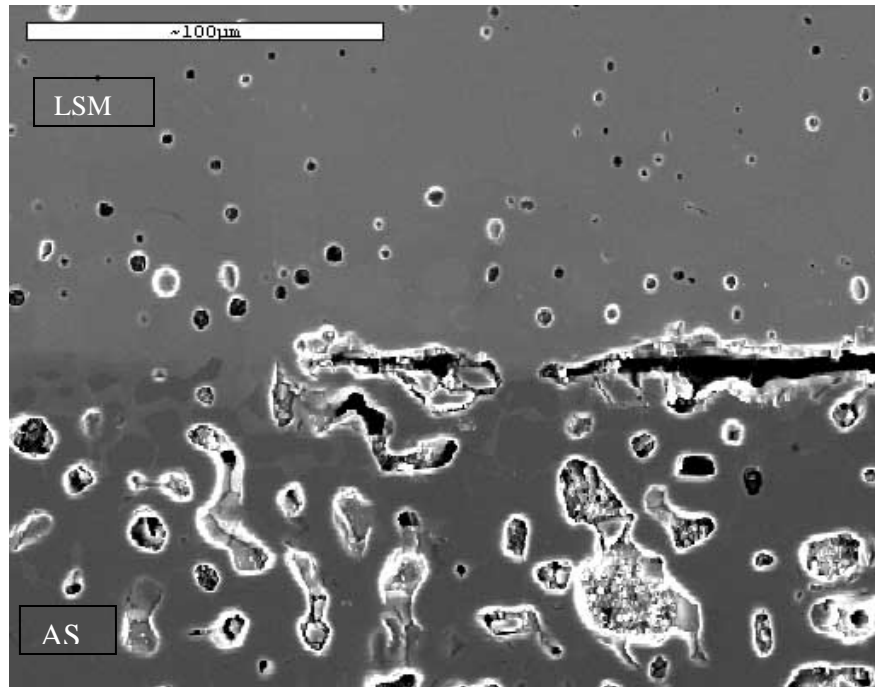


Figure 8. SEM of the cross section of the bi-layer IC